Novel Glass-Forming Organic Materials. 3. Cubane with Pendant Nematogens, Carbazole, and Disperse Red 1

Shaw H. Chen,*,†,‡ John C. Mastrangelo,† Hongqin Shi,† Thomas N. Blanton,§ and A. Bashir-Hashemi||

Materials Science Program and Chemical Engineering Department, and Laboratory for Laser Energetics, Center for Optoelectronics & Imaging, 240 East River Road, University of Rochester, Rochester, New York 14623-1212, Analytical Technology Division, Eastman Kodak Company, Kodak Park, BLDG. 49, Rochester, New York 14652-3712, and Geo-Centers, Inc., at Armament Research, Development and Engineering Center, Lake Hopatcong, New Jersey 07849

Received July 26, 1996; Revised Manuscript Received November 4, 1996[⊗]

ABSTRACT: Mesogenic and nonmesogenic functional moieties were attached as pendant groups to the cubane core for an investigation of the glass-forming ability and morphological stability of the hybrid systems. Nematogens and carbazole were found to yield hybrid systems that are nematic and isotropic, respectively, all capable of vitrification with above-ambient glass transition temperatures (T_gs). Moreover, DR1 was found to yield a hybrid system possessing S_A mesomorphism upon thermal processing under kinetically controlled conditions; it was further demonstrated that S_A glass could be obtained with a T_g of 95 °C. On the other hand, crystals were obtained with thermal processing under thermodynamically controlled conditions. Of the five model compounds based on cubane, it appears that the lower the melting or clearing temperature of the pendant group, the more morphologically stable the hybrid system. It was also found that adamantane-based systems possess about the same T_g with a superior morphological stability in comparison to the cubane-based counterparts.

I. Introduction

Organic materials containing appropriate functional moieties, both polymeric and low molar mass in structure, hold promise for various applications to optics, electronics, and optoelectronics. Although single crystallinity is normally preferred in practical applications, the difficulty (and hence the prohibitively high cost) encountered in processing them into thin films has rendered "glass" a morphology of choice. Whereas vitrification appears to be a privilege of polymeric materials, their generally high melt viscosity and broad distribution of relaxation times have been recognized as potential problems where processing into large-area thin films is desired. In view of the ease with which thin films can be prepared with molecular (*i.e.*, low-molar-mass) materials, our recent effort has focused on the design, synthesis, and characterization of both mesogenic and isotropic organic systems.[1−5] In principle, all liquids should vitrify given a sufficiently rapid cooling rate. However, thermally-induced phase transformation may occur in view of the nonequilibrium vitreous state. Nevertheless, both vitrification of organic materials and morphological stability of resultant glasses have remained largely poorly understood from the perspective of chemical structure. Furthermore, the design of vitrifiable liquid crystals with an elevated glass transition temperature (T_g) is particularly challenging in that a subtle structural balance must be struck between *order* (*i.e.*, liquid crystalline mesomorphism) and *disorder* (*i.e.*, glass).

In a recent series of studies,[1−5] we have explored a generic and yet simplistic molecular design approach in which functional moieties, including mesogenic ones, are chemically bonded to a ring structure serving as a volume-excluding core. The idea is to have these two structural elements present an excluded-volume effect on each other for the promotion of glass formation and morphological stability against recrystallization. It was found that cyclohexane, bicyclooctene, and adamantane with mesogenic as well as nonmesogenic pendant groups are capable of vitrification. Moreover, it was found that morphological stability is a consequence of the partial coupling between the central core and the pendant group provided by a flexible spacer connecting the two. The present work was motivated by the desire to further explore organic glass-formers in light of the facts that four mesogens emanating from a central carbon atom fail to vitrify,[6] that silsesquioxanes with pendant mesogens form unstable glasses,[7] and that dendrimers of up to four generations are capable of forming mesomorphic glasses.[8,9] To gain a broader perspective on vitrifiable organic materials, cubane with pendant mesogenic and nonmesogenic groups were synthesized for characterization by hot-stage polarized optical microscopy (POM), differential scanning calorimetry (DSC), and X-ray diffractometry (XRD). Of particular interest is the effect of having four pendant groups configured into a tetrahedral orientation on vitrification and liquid crystalline mesomorphism.

II. Experimental Section

Reagents and Chemicals. All solvents and reagents were used as received from Aldrich Chemical Co. or J. T. Baker with the exception of tetrahydrofuran, which was dried by refluxing over sodium in the presence of benzophenone until blue and then collected via distillation.

Material Synthesis. 1,3,5,7-tetrakis(chlorocarbonyl)cubane. Based on the procedures reported by Eaton *et al.*[10] partial saponification of 1,4-bis(methoxycarbonyl)cubane and the subsequent Barton decarboxylation were carried out to yield cubanecarboxylic acid, which was then converted to 1,3,5,7-tetrakis(chlorocarbonyl)cubane via photochemical chlorocarbonylation.[11] The overall yield was 34%.

* Author to whom correspondence should be addressed.
† Materials Science Program and Chemical Engineering, University of Rochester.
‡ Laboratory for Laser Energetics, University of Rochester.
§ Eastman Kodak.
|| Geo-Centers, Inc.
⊗ Abstract published in *Advance ACS Abstracts,* December 15, 1996.

S0024-9297(96)01115-1 CCC: $14.00

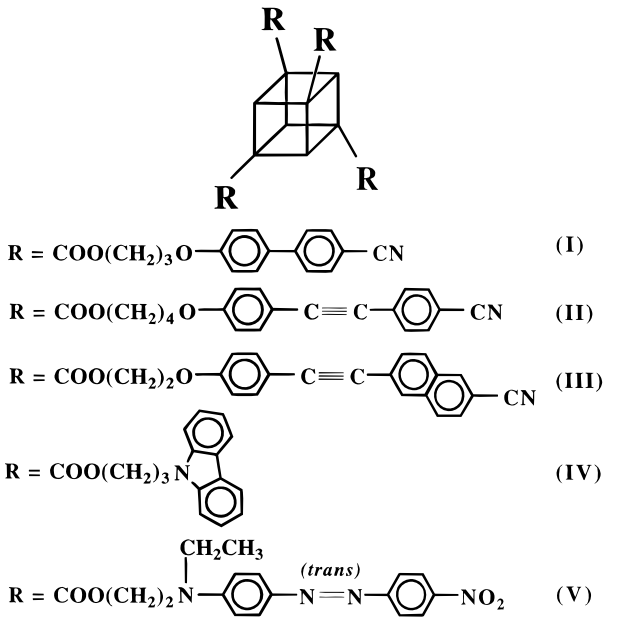

Figure 1. Chemical structures of compounds **I**−**V**.

Model compounds **I**−**V**, as depicted in Figure 1, were synthesized for the present study by reacting 1,3,5,7-tetrakis-(chlorocarbonyl)cubane with a series of precursor alcohols: 3-[[4-(4′-cyanobiphenyl)yl]oxy]propanol (I 111 °C N on cooling), 4-[4-[(4-cyanophenyl)ethynyl]phenoxy]butanol (K 132 °C N 146 °C I), 2-[4-[(2-(6-cyanonaphthyl))ethynyl]phenoxy]ethanol (K 178 °C N 242 °C I), 3-(*N*-carbazolyl)propanol (K 104 °C I), and 2-[*N*-[4-[(4-nitrophenyl)azo)]phenyl]-*N*-ethylamino]ethanol (*i.e.* Disperse Red 1, or DR1, K 165 °C I). The synthesis and purification of all these alcohols have been reported previously,[2,4,12,13] and their thermal transition temperatures determined with DSC are reported here with the following symbols: K, crystalline; N, nematic; I, isotropic. The synthesis of model compounds was accomplished following formerly reported procedures.[3]

Characterization Techniques. A Hitachi high-performance liquid chromatography (HPLC) system comprising an L-2000 metering pump and an L-4200 UV-Vis absorbance detector equipped with an LiChrosorb column (RP-18, 10 μm) was employed to determine the number of components and purity of the intermediates and products. The purity levels of all final products were found to be better than 99% based on HPLC analysis. Chemical structures were elucidated with elemental analysis (performed by Oneida Research Services, Inc., Whitesboro, NY) and FTIR (Nicolet 20 SXC) and proton NMR (QE-300, GE) spectroscopic techniques.

Thermal transition temperatures were determined by DSC (Perkin-Elmer DSC-7) with a continuous nitrogen purge at 20 mL/min. A heating rate of 20 °C/min was normally employed to gather a thermogram with DSC unless noted otherwise. A DuPont 951 thermogravimetric analyzer interfaced with a DuPont Thermal Analyst 2100 System was used to perform a TGA experiment at a nitrogen purge of 50 mL/min and a scan rate of 20 °C/min. Morphology and liquid crystallinity were identified with a polarized optical microscope (Leitz Orthoplan-Pol), equipped with a hot stage (FP82, Mettler) plus a central processor (FP80, Mettler).

The X-ray diffraction data were collected in reflection mode using a Siemens θ/θ Bragg-Brentano diffractometer utilizing nickel-filtered Cu radiation and a Braun position sensitive detector set to measure Cu Kα radiation. Two-dimensional flat-plate diffraction data were collected using Cu Kα radiation, image-plate detector, and a sample to film distance of 5−17 cm. Samples in the form of powder, pellet, or drawn fiber were employed.

III. Results and Discussion

The five model compounds synthesized for the present study are depicted in Figure 1 as **I**−**V** with their chemical structures validated by elemental analysis and proton-NMR spectral data, compiled in Tables 1 and 2, respectively. Since thermal transition temperatures as determined by DSC are normally functions of prior thermal treatment and scanning rate as well, a consistent procedure was followed in which a sample was heated to beyond T_c (clearing temperature) or T_m (melting temperature), whichever is applicable, followed by quenching at −200 °C/min to −30 °C before gathering a heating scan at 20 °C/min. Because of the relatively high transition temperatures encountered in **III** and **V**, TGA experiments were performed to establish the thermal stability of both compounds up to 250 °C. The DSC heating scans of the quenched **I** through **IV** reproduced in Figure 2 suggest the morphological stability of nematic, identified as threaded textures, and isotropic melts against thermally activated recrystallization in the case of **I**, **II**, and **IV** but a tendency of the nematic melt of **III** to recrystallize on heating. A more systematic test of morphological stability was conducted by heating quenched samples at a decreasing heating rate, thus allowing more time for recrystallization to occur. The morphological instability will manifest itself in the appearance of a recrystallization exotherm and/

Table 1. Elemental Analysis of Compounds I−V

compd		C %	H %	N %
I	calcd	74.74	4.95	4.59
	obsd	74.20	4.97	4.38
II	calcd	76.95	4.99	4.08
	obsd	76.40	4.75	4.09
III	calcd	78.89	4.14	3.83
	obsd	78.06	4.55	3.74
IV	calcd	77.96	5.45	5.05
	obsd	77.58	5.46	4.95
V	calcd	62.29	4.95	15.29
	obsd	62.05	5.10	15.43

Table 2. Proton NMR Spectral Data for Compounds I, II, IV, and V in $CDCl_3$ and for Compound III in Dimethyl sulfoxide-d_6

δ, ppm	assignment
	Compound **I**
7.84−6.94	m, 32 H, aromatic
4.66	s, 4 H, cubane
4.39	t, 8 H, $COOCH_2CH_2$
4.08	t, 8 H, CH_2CH_2O
2.18	p, 8 H, $CH_2CH_2CH_2$
	Compound **II**
7.82−6.81	m, 32 H, aromatic
4.67	s, 4 H, cubane
4.26	t, 8 H, $COOCH_2CH_2$
4.02	t, 8 H, CH_2CH_2O
1.92	m, 8 H, $CH_2CH_2CH_2$
	Compound **III**
8.50−6.50	m, 40 H, aromatic
4.50	s, 4 H, cubane
4.43	t, 8 H, $COOCH_2CH_2$
4.22	t, 8 H, CH_2CH_2O
	Compound **IV**
8.12−7.20	m, 32 H, aromatic
4.80	s, 4 H, cubane
4.40	t, 8 H, CH_2CH_2N
4.18	t, 8 H, $COOCH_2CH_2$
2.27	p, 8 H, $CH_2CH_2CH_2$
	Compound **V**
8.39−6.68	m, 32 H, aromatic
4.54	s, 4 H, cubane
4.36	t, 8 H, $COOCH_2CH_2$
3.66	t, 8 H, CH_2CH_2N
3.48	q, 8 H, NCH_2CH_3
1.24	t, 12 H,CH_2CH_3

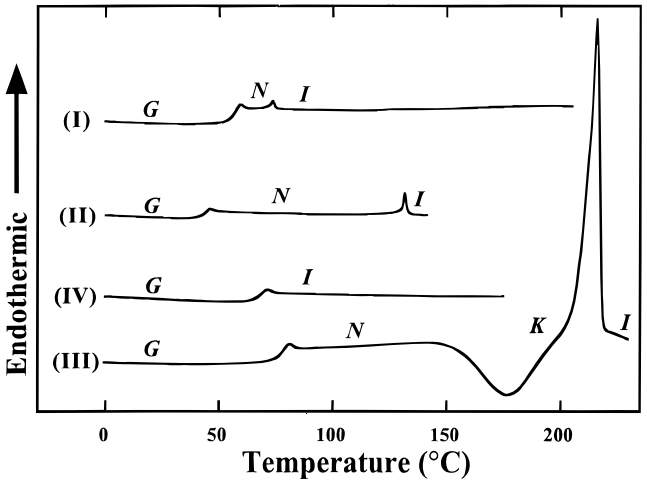

Figure 2. DSC thermograms of compounds **I**−**IV** at 20 °C/min; samples were preheated to 220 °C followed by quenching at −200 °C/min to −30 °C. Symbols: K, crystalline; G, glassy; N, nematic; and I, isotropic.

or a melting endotherm of resultant crystals on heating from below T_g. It was found that heating quenched **II** or **IV** at a rate down to 0.2 °C/min produced no evidence of instability, whereas heating **I** at 2 °C/min resulted in a visible melting endotherm. Therefore, the morphological stability against thermally activated recrystallization follows the decreasing order: **II** ≈ **IV** > **I** > **III**. As a comparison, we note that the adamantane equivalent of **III** showed the same T_g of 77 °C with an improved morphological stability in that no recrystallization was observed on heating at the same rate of 20 °C/min. The fact that nematic mesomorphism was observed in **I**−**III** indicates that the four pendant groups connected via a flexible spacer to a given cubane core align unaxially with those on neighboring cubane cores, as in the case of adamantane serving as the central core.[3]

Compound **V** turned out to be quite rich in its morphological characteristics. As its pristine sample was heated at 20 °C/min to 220 °C, an exothermic solid-solid transition took place, resulting in crystal K_1 (T_{m1} = 185 °C with ΔH_{m1} = 61 J/g on heating) with traces of a higher melting crystal K_2 (see Figure 3a). On the basis of this observation, crystal K_1 was produced by heating a pristine sample of **V** to 150 °C, followed by quenching to room temperature for gathering the XRD pattern shown in Figure 4a. To produce crystal K_2, a pristine sample of **V** was thermally cycled between −30 and 200 °C three times, as monitored in Figure 3b. As shown by the second, third, and fourth heating scans (i.e. scans 2−4 in Figure 3b), thermal cycling between −30 and 200 °C accomplished a depletion of crystal K_1. Indeed, scan 5 verifies that crystal K_2 (T_{m2} = 210 °C with ΔH_{m2} = 75 J/g on heating) was successfully produced, and its XRD pattern shown Figure 4b is distinct from that shown in Figure 4a, *i.e.* that of crystal K_1. On the other hand, thermally cycling a pristine sample of **V** between −30 and 220 °C up to six times was found to produce a liquid crystalline glass (T_g = 95 °C with ΔC_p = 0.31 J/g·°C and T_c = 155 °C with ΔH_c = 15 J/g on heating) with traces of crystal K_1, as demonstrated in Figure 5, with phase identification to be elaborated in what follows.

To identify the type of the resultant mesomorphism, a thin film of the thermally cycled sample of **V** was prepared between a pair of microscope glass slides, and the focal conic fan textures observed with polarized optical microscopy, as shown in Figure 6, were found to clear upon heating at 5 °C/min to 152 °C on a hot stage, which is in agreement with the DSC data. The

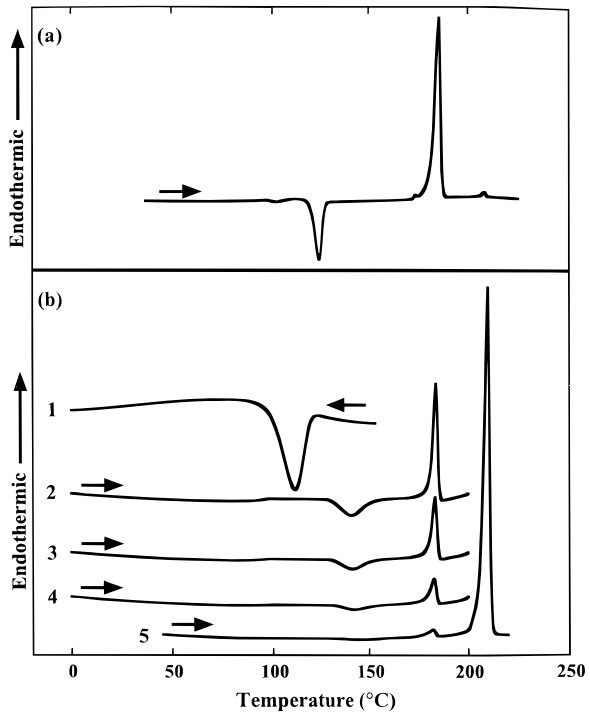

Figure 3. (a) DSC heating scan of pristine **V** to 220 °C at 20 °C/min. (b) DSC thermograms of **V** at 20 °C/min unless noted otherwise: 1, quenching scan of sample preheated to 200 °C; 2, heating scan after quenching, scan 1; 3, heating scan upon quenching following scan 2; 4, heating scan upon quenching following scan 3; 5, heating scan upon quenching following scan 4. Note that no time elapsed between heating and quenching scans.

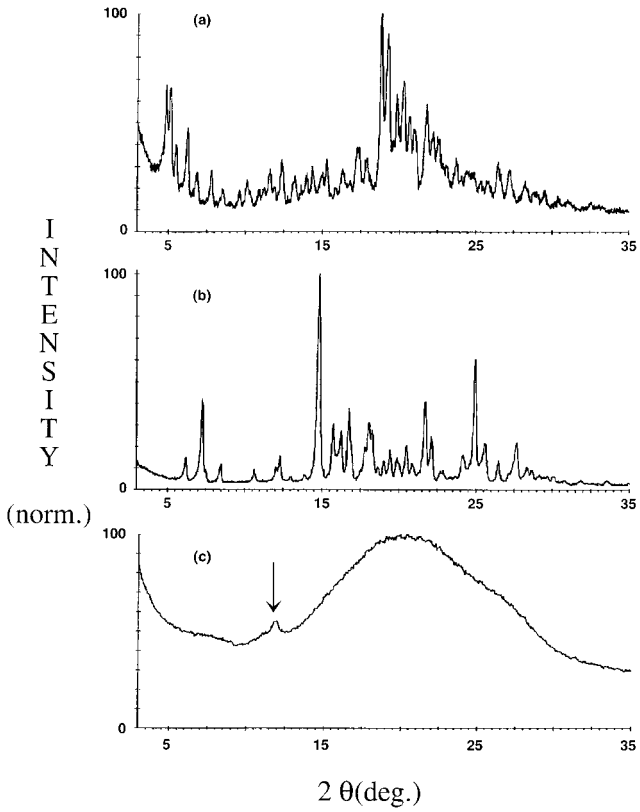

Figure 4. XRD pattern of (a) crystal K_1, (b) crystal K_2, and (c) S_A glass. All three samples were obtained via thermal treatment as described in the text.

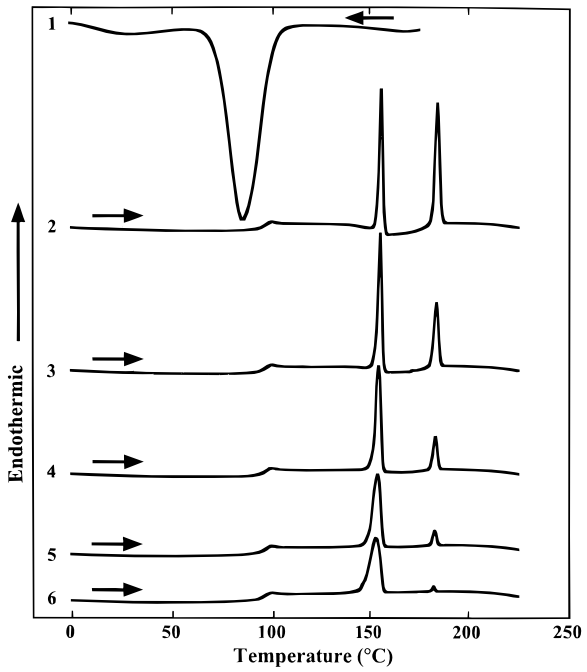

Figure 5. DSC monitoring of thermal cycling that produced S_A glass from **V** with all heating scans performed at 20 °C/min: 1, quenching scan of sample preheated to 220 °C; 2, heating scan after quenching scan 1; 3, heating scan upon quenching following scan 2; 4, heating scan upon quenching following scan 3; 5, heating scan upon quenching following scan 4; 6, heating scan upon quenching following scan 5. Note that no time elapsed between heating and quenching scans.

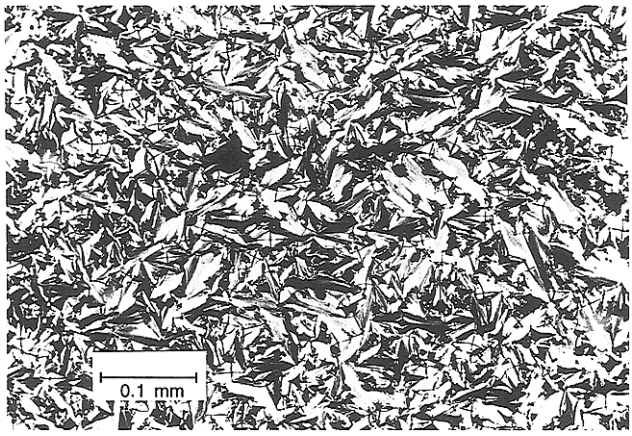

Figure 6. Polarized optical micrograph of an S_A glass produced from **V** following thermal cycling as represented in Figure 5 at a magnification factor of 200.

same samples in pellet and oriented fiber were further investigated by XRD. The diffraction peak at $2\theta = 11.9°$ in Figure 4c corresponds to an interplanar spacing of 7.4 Å, which may be due to a second-order layer line. Windle[14] and Kosaka and Uryu[15] have described diffraction patterns similar to the one observed in Figure 4c as representative of an S_A type liquid crystal. To further support this interpretation, an oriented sample of **V** was prepared by drawing a fiber from the melt of a pellet processed identical to the one analyzed in Figure 4c. The flat-plate diffraction pattern of this fiber, shown in Figure 7, reveals the orientation achieved by drawing with a strong axial diffraction signal and equatorial arcs. These arcs correspond to a *d*-spacing of 7.4 Å, which is the same interplanar spacing as observed for the peak noted in Figure 4c. The pattern revealed in Figure 7 is consistent with an oriented S_A type liquid

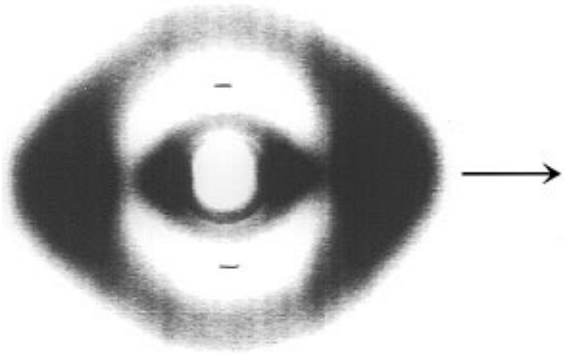

Figure 7. Flat-plate diffraction pattern of a fiber drawn from an S_A glass above its T_g produced from **V** following thermal cycling as represented in Figure 5.

crystal, although the morphological significance of the 7.4 Å peak is not clear at this time.

It was a little surprising to observe S_A mesomorphism in **V** in view of the facts that DR 1 is nonmesogenic in its pure form and that **I**−**III** containing nematogenic pendants are capable of nematic mesomorphism. Furthermore, to the best of our knowledge there exist no known DR1-containing compounds that are mesomorphic.[3,4] As suggested by scan 2 in Figure 3b or scan 2 in Figure 5, thermally quenched **V** lacks morphological stability in view of the evidence of recrystallization upon heating at 20 °C/min. It is noted that although nonmesogenic, the adamantane equivalent of **V** showed a T_g of 90 °C with a superior morphological stability.[3] Therefore, on the scale of morphological stability, **V** is equivalent to **III**, both being the worst of all five model compounds. Even so, the S_A mesomorphism produced under kinetically controlled conditions and frozen in a glassy matrix showed no evidence of recrystallization when left at room temperature for months (and perhaps years as time permits). From the standpoint of chemical structure, it appears that the higher the T_c or T_m of the precursor alcohol (as reported in the Experimental Section), the less morphologically stable the hybrid system (*i.e.* cubane with four identical pendant groups).

Having isolated the three morphologies from **V** via thermal processing, let us examine the underlying processes. As shown in Figure 3, quenching a sample preheated to 200 °C resulted in an exotherm (scan 1 of Figure 3b), presumably giving rise to a mixture of crystals K_1 and K_2 plus glass below T_g. Subsequent thermal cycling between −30 and 200 °C (scans 2−4 in Figure 3b) led to an increasing amount of crystal K_2. Note the decreasing ΔC_p associated with the glass transition (0.18, 0.08, and 0.03 J/g·°C for scans 3, 4, and 5, respectively), the decreasing recrystallization endotherm at 142 °C (12.1, 7.8, and 3.9 J/g for scans 3, 4, and 5, respectively), and the decreasing amount of crystal K_1 as determined by the melting enthalpy at 185 °C (21.6, 13.2, and 6.2 J/g for scans 3, 4, and 5, respectively, compared to 61 J/g for pure K_1) as thermal cycling proceeded. It is evident that recrystallization of the melt led to both K_1 and K_2, and the portion of the material ending up in K_2 stayed in that form because the heating cycle did not melt K_2. Ultimately, a complete conversion into crystal K_2 is expected, as evidenced by scan 5 of Figure 3. Alternatively, thermal annealing at a temperature between T_{m1} and T_{m2} should ultimately yield pure K_2.

As a pristine sample of **V** was heated to 220 °C and then quenched to −30 °C, a mixture of K_1, S_A, and glass emerged as identified with POM and XRD. Thermal

cycling between −30 and 220 °C followed, and the heating scans shown in Figure 5 suggest that residual crystal K_1 was converted into S_A, while the value of ΔC_p associated with glass transition was found to stay constant at 0.34 ± 0.02 J/g·°C. Thermally cycled **V** was recovered for analysis by proton-NMR and FTIR to confirm its chemical integrity. It appears that S_A is a kinetically favored product of thermal cycling. The fact that the melting endotherm of the thermodynamically favored crystal K_1 decreased as thermal cycling proceeded suggests the diminishing nucleation sites for K_1 to grow as a result of heating above T_{m1}. At the same time, the enthalpy associated with the clearing of S_A was found to increase steadily from 14.9 to 16.4 J/g for heating scans 2−6 in Figure 5. In contrast, one would expect thermal annealing at an elevated temperature over an extended period of time to yield thermodynamically favored crystals K_1 and K_2. An extension of this argument is that one should be able to observe nematic mesomorphism, which is less energetically favored than S_A, under proper kinetically controlled conditions. One remaining question is, why did S_A not appear in the DSC scans shown in Figure 3b? It is speculated that the upper limit of thermal cycling, 200 °C, is so close to the melting point of crystal K_1, 185 °C, that its nucleation sites remain largely intact. As a result, recrystallization of the melt to form K_1 is much favored over the formation of S_A. The presently demonstrated ability to isolate three phases, K_1, K_2, and S_A, by thermal processing does suggest that one should be cautious about the phase behavior of liquid crystalline materials as normally determined by a combination of POM and DSC under kinetically controlled conditions.

IV. Conclusions

As part of our continuing effort targeting vitrifiable molecular materials, an intermediate 1,3,5,7-tetrakis-(chlorocarbonyl)cubane was employed to synthesize hybrid systems containing pendant nematogenic, carbazolyl, and DR1 groups. Unlike their polymeric counterparts, these compounds possess well-defined molecular structure carrying no chain ends or molecular weight distribution. However, they resemble polymeric materials in their ability to vitrify and to form films or fibers to facilitate practical applications. The thermotropic property and morphological stability of the products were characterized using the DSC, POM, and XRD techniques, leading to the main observations as recapitulated below.

(1) Although the pendant nematogens, carbazole, and DR1 are all highly melting crystals, their hybrids with cubane, which is also crystalline on its own, were found to be capable of vitrification with above-ambient T_gs.

(2) Cubane with four pendant DR1 groups turned out to be an interesting systems in that S_A glass was obtained via thermal processing under kinetically controlled conditions, whereas crystals were obtained under thermodynamically controlled conditions.

(3) Morphological stability of the cubane-based hybrid systems against thermally activated recrystallization was found to increase with decreasing T_m or T_c of the pendant group.

(4) For a given pendant group, adamantane as the central core produces a hybrid system with roughly the same T_g as cubane but an improved morphological stability.

Acknowledgment. We thank Professor A. S. Kende of the Chemistry Department at the University of Rochester for assistance in organic synthesis, K. L. Marshall, A. Schmid, and S. D. Jacobs of the Laboratory for Laser Energetics for helpful discussions. We would like to express our gratitude for the financial support provided by the Ministry of International Trade and Industry of Japan and the National Science Foundation under Grant CTS-9500737 and Equipment Grant CTS-9411604. In addition, our advanced organic materials research was supported in part by the U.S. Department of Energy Office of Inertial Confinement Fusion under Cooperative Agreement No. DE-FC03-92SF19460, the University of Rochester, and the New York State Energy Research and Development Authority. Financial support provided by Armament Research, Development and Engineering Center to Geo-Centers, Inc., is also gratefully acknowledged.

References and Notes

(1) Shi, H.; Chen, S. H. *Liq. Cryst.* **1995**, *19*, 849.
(2) Shi, H.; Chen, S. H. *Liq. Cryst.* **1995**, *18*, 733.
(3) Chen, S. H.; Mastrangelo, J. C.; Shi, H.; Bashir-Hashemi, A.; Li, J.; Gelber, N. *Macromolecules* **1995**, *28*, 7775.
(4) Mastrangelo, J. C.; Chen, S. H.; Blanton, T. N. *Chem. Mater.* **1995**, *7*, 1904.
(5) Chen, S. H.; Mastrangelo, J. C.; Blanton, T. N.; Bashir-Hashemi, A.; Marshall, K. L. *Liq. Cryst.* In press.
(6) Zab, K.; Joachimi, D.; Agert, O.; Neumann, B.; Tschierske, C. *Liq. Cryst.* **1995**, *18*, 489.
(7) Kreuzer, F.-H.; Maurer, R.; Spes, P. *Makromol. Chem., Makromol. Symp.* **1991**, *50*, 215.
(8) Percec, V.; Chu, P.; Ungar, G.; Zhou, J. *J. Am. Chem. Soc.* **1995**, *117*, 11441.
(9) Lorenz, K.; Hölter, D.; Stühn, B.; Mülhaupt, R.; Frey, H. *Adv. Mater.*, **1996**, *8*, 414.
(10) Eaton, P. E.; Nordari, N., Tsanaktsidis, J.; Upadhyaya, S. P. *Synthesis* **1995**, 501.
(11) (a) Bashir-Hashemi, A. *Angew. Chem. Int. Ed. Engl.* **1993**, *32*, 612. (b) Bashir-Hashemi, A.; Li, J.; Gelber, N.; Ammon, H. *J. Org. Chem*. **1995**, *60*, 698.
(12) Shi, H.; Chen, S. H. *Liq. Cryst.* **1994**, *17*, 413.
(13) Mastrangelo, J. C.; Conger, B. M.; Chen, S. H.; Bashir-Hashemi, A. *Chem. Mater.* Accepted.
(14) Windle, A. H. *Liquid Crystalline and Mesomorphic Polymers*; Shibaév, V. P. Lam, L., Eds.; Springer-Verlag: New York, 1994; p 69.
(15) Kosaka, Y.; Uryu, T. *J. Polym. Sci., Pt. A, Polym. Chem*. **1995**, *33*, 2917.

MA961115J